HUMAN VACCINES & IMMUNOTHERAPEUTICS
2020, VOL. 16, NO. 9, 2042–2050
https://doi.org/10.1080/21645515.2020.1793711

Taylor & Francis
Taylor & Francis Group

RESEARCH PAPER

OPEN ACCESS Check for updates

Immune-engineered H7N9 influenza hemagglutinin improves protection against viral influenza virus challenge

Hyesun Jang[a,b], Lauren M. Meyers[c], Christine Boyle[c], Anne S. De Groot[c,b], Lenny Moise[d,c], and Ted M. Ross[a,b]

[a]Department of Infectious Diseases, University of Georgia, Athens, GA, USA; [b]Center for Vaccines and Immunology, University of Georgia, Athens, GA, USA; [c]EpiVax, Providence, RI, USA; [d]Institute of Immunology and Informatics, Department of Cell and Molecular Biology, University of Rhode Island, Providence, RI, USA

ABSTRACT

The influenza hemagglutinin (HA) isolated from avian H7N9 influenza virus strains elicit weak immune responses. This low immunogenicity may be due to a regulatory T cell (T_{reg})–stimulating epitopes in HA from the H7N9 isolate A/Anhui/1/2013 (Anh/13). In this report, this T_{reg} stimulating sequence was removed from the wild-type (WT) H7 HA amino acid sequence and replaced with a conserved CD4 + T cell stimulating sequences from human seasonal H3N2 strains and designed OPT1 H7 HA. The effectiveness of this optimized H7 HA protein was determined using a humanized mouse (HLA-DR3) expressing the human leukocyte antigen (HLA) DR3 allele. HLA-DR3 mice were pre-immunized by infecting with H3N2 influenza virus, A/Hong Kong/4108/2014 and then vaccinated intramuscularly with either the WT H7 HA from Anh/13 or the OPT1 H7 HA antigen without adjuvant. The OPT1 H7 HA vaccination group elicited higher H7 HA-specific IgG titers that resulted in a lower mortality, weight loss, and lung viral titer following lethal challenge with the H7N9 Anh/13 influenza virus compared to WT-vaccinated mice. Overall, T-cell epitope-engineered vaccines can improve the immunogenicity of H7 HA antigens resulting in enhanced survival and lower morbidity against H7N9 influenza virus challenge.

ARTICLE HISTORY
Received 23 April 2020
Revised 22 June 2020
Accepted 1 July 2020

KEYWORDS
Asian H7N9; pandemic influenza vaccine; T cell epitope engineering; humanized mouse model

Introduction

Asian lineage avian influenza H7N9 virus infected ~1565 people from 2013 to 2017 with a 39% case-fatality rate[1]. Since 2019, there have been no additional reported human infections[1], but H7N9 influenza viruses continue to circulate in animal reservoirs. Since the H7N9 influenza viruses are of moderate to high risk to initiate an influenza pandemic, various world governments are stockpiling H7N9 viruses to accelerate vaccine production in the future.[2] However, the effectiveness of currently available H7N9 influenza vaccines is poor, requiring at least two doses with the maximum amount of antigen, plus adjuvant, to elicit a protective immune response.[3] For prompt production and distribution during an emergency, an H7N9 influenza virus vaccine that is effective following a single, minimum dose of vaccine is desired.

The avian H7N9 influenza HA protein has a substantially lower frequency of $CD4^+$ T-cell epitopes than HA antigens from seasonal influenza strains.[4] Although epitopes cross-conserved with seasonal influenza are present in H7 HA,[5] they do not sufficiently mobilize the memory compartment to support a strong immune response to the novel HA antigen. Furthermore, the H7 HA protein was predicted to contain a regulatory T cell (T_{reg}) stimulating epitope.[6] Incorporation of human-like epitopes capable of activating T_{regs} is a mechanism of viral 'camouflage', known as antigenic mimicry, which permits escape from targeted human immune responses.[6] T_{reg} epitope activated human $CD4^+CD25^{high}CD39^+FoxP3^+$ regulatory T cells suppress H7N9 influenza virus-specific peripheral effector interferon gamma positive T cell responses. In order to enhance H7 HA vaccines, T cell epitopes were added to the HA antigen to trigger a rapid recall response from preexisting seasonal influenza-specific memory T cells.[7] Approximately ~67% (6 of 9 residues) of the amino acids in the T_{reg} epitopes aligned between the H7 and H3 HA antigens. However, this highly conserved epitope in seasonal H3N2 viruses activates effector, rather than regulatory T cells. Therefore, with minimal changes to the H7 HA amino acid sequence, the T_{reg} epitope was removed and a $CD4^+$ T-cell stimulating epitope was added simultaneously. The optimized sequence was expressed as recombinant protein (OPT1 H7 HA) and initially evaluated for its immunogenicity in NOD/SCID/JAK3 (null) immunodeficient mice that were reconstituted with human peripheral blood mononuclear cells (PBMC).[6] Following vaccination, OPT1 H7 HA vaccinated mice had greater than a four-fold increase in HA-specific IgG titers compared to donor-matched mice vaccinated with WT H7 HA vaccine.[8]

Our current study investigated whether these enhanced immune responses can better protect against a lethal challenge with avian H7N9 influenza virus. To eliminate the variation introduced through PBMC donor-history, a humanized mouse model of major histocompatibility complex (MHC)-II knockout/HLA-DR knock-in transgenic mice (HLA-DR3) was used to emulate human MHC-II mediated T cell responses. In addition, the HLA-DR3 transgenic mice were pre-immunized with a non-lethal dose of seasonal H3N2 virus via intranasal infection to naturally develop H3 HA-specific T cell immunity that could be recruited to boost H7 HA responses.

CONTACT Ted M. Ross tedross@uga.edu Center for Vaccines and Immunology, University of Georgia, 501 D.W. Brooks Drive, CVI Room 1504, Athens, GA 30602, USA

Materials and methods

Vaccine preparation

The amino acid sequence of the influenza A/Anhui/1/2013 H7 HA [H7 sequence identical to A/Shanghai/02/2013 H7N9;[9] Accession: YP_009118475] was obtained from GenBank (www.ncbi.nlm.nih.gov). The OPT1 H7 HA design was produced using the iVAX T cell epitope discovery and vaccine design immunoinformatic platform, as previously described.[8,10] Three amino acid changes were made from 320-**RSLL**-323 (WT) to 320-**NTLK**-323 (OPT1), as indicated in bold (Figure 1B).

The wild type and OPT1 H7 HA ectodomains were expressed as soluble trimeric recombinant proteins (H7 rHAs). Briefly, the transmembrane and intracellular regions of the HA sequence were replaced with a $(GS)_3$ linker followed by the GCN4 trimerization domain,[11] Avi Tag™, a glycine residue, and finally a 6X HIS tag (Figure 1B).[12] The amino acid sequences were reverse translated and optimized for expression in mammalian cells, including codon usage and RNA sequence optimization (Genewiz, Washington, DC, USA). The final sequences were inserted into pcDNA3.1/Zeo (+) using HindIII and EcoRI restriction enzyme sites and verified by sequencing (Genewiz, South Plainfield, NJ, USA). Plasmids were amplified in *Escherichia coli* (strain DH5-alpha) and purified using QIAGEN plasmid maxi kit, according to the manufacturer's protocol. Plasmids were verified using restriction enzyme digests and resolved on a 1% agarose gel, viewed with SYBR safe under UV light. The H7 rHAs were transiently expressed in Expi293 suspension cells using the ExpiFectamine™ 293 Transfection Kit (Thermo Fisher Scientific; Pittsburgh, PA, USA). After incubation for 3 d at 37°C, supernatant was harvested and H7 rHAs were purified via a C-terminal histidine tag using HisTrap excel nickel affinity chromatography columns (GE Healthcare Life Sciences, Marlborough, MA, USA). Protein concentration was determined by MicroBCA™ Protein Assay Kit (Thermo Fisher Scientific; Pittsburgh, PA, USA).

Native blue PAGE

To confirm whether the proteins were correctly folded in trimeric form, native PAGE protein separation was performed according to the protocol provided by the gel manufacturer (Thermo Fisher Scientific, Waltham, MA, USA). Briefly, 5 µg of the purified proteins was prepared under native conditions (mixed with NativePAGE™ Sample Buffer (4X), 1% DDM (n-dodecyl-β-D-maltoside), NativePAGE™ 5% G-250 Sample Additive). Electrophoresis was carried out using a NativePAGE™ Novex® 3–12% Bis-Tris gel at 150 V and 80 mA for 1 h. The gel was destained with a Methanol-Acetate-Water mixture (45:10:45) overnight.

SDS-PAGE and western blotting

All H7 rHAs were confirmed by Western blotting similarly to previously described protocols.[13] In brief, rHAs (0.2 µg) were electrophoresed along with the same amount of standard recombinant antigen (H1N1 A/California/07/2009) on a 10% Bis-Tris SDS-PAGE (Thermo Fisher Scientific, Waltham, MA) and transferred to a PVDF membrane using the Trans-Blot Turbo Transfer System (Bio-Rad, Hercules, CA), per manufacturer instructions. The blot was probed with purified anti-His Tag primary antibody (clone J099B12; BioLegend®, San Diego, CA), and HRP-conjugated anti-mouse IgG (Southern Biotech, Birmingham, AL) secondary Ab. Images were collected using the iBind Western Device (Thermo Fisher Scientific).

Mouse study

HLA-DR3 mice were obtained from Dr. Chella David (Mayo Medical School) under a commercial license and material transfer agreement. The mice express the HLA DR3α and β genes on a B.10-Ab^0 mouse class II-negative background. Mice (n = 43; female, 6–8 weeks) were shipped from the EpiVax colony at Taconic Bioscience (Rensselaer, NY, USA) to the University of Georgia and divided into five groups (Figure 2). All mice were housed in microisolator units and allowed free access to food and water and were cared for under USDA guidelines for laboratory animals. Upon arrival, all mice were bled to confirm seronegative to influenza A/Anhui/1/2013 (H7N9) and A/Hong Kong/4108/2014 (H3N2) viruses.

Twelve mice designated as the naïve control group were not infected or immunized but were the challenged. The remaining 31 mice were infected intranasally (1X10^6 PFU/

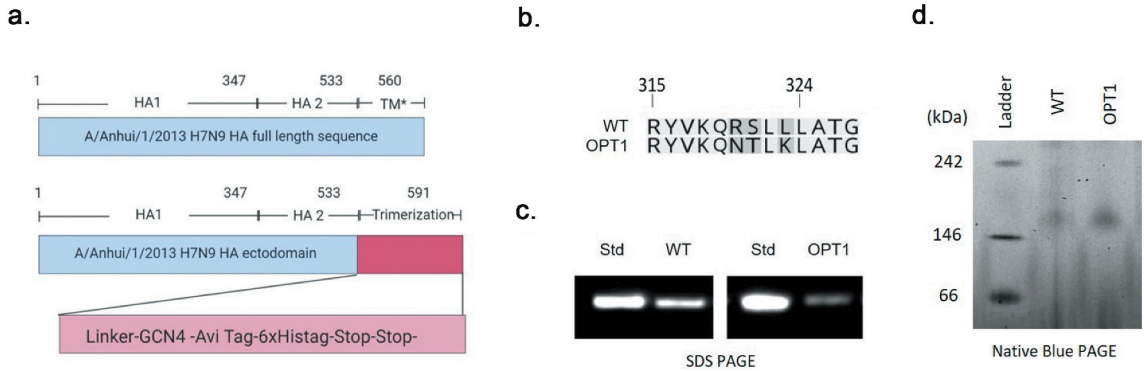

Figure 1. Vaccine preparation. OPT1 H7 rHA was designed by substitution of 3 amino acids of wild-type H7 rHA(A). This modified HA sequence was expressed as a trimeric soluble recombinant HA protein (H7 rHA) by replacing the transmembrane domain with a trimerization domain (B). The expression of H7 rHA was confirmed by anti-his *taq* western blot analysis (C) and native blue PAGE was conduced to confirm the trimeric forms (D) *WT: WT H7 rHA, OPT1: OPT1 H7 rHA,, TM*: transmembrane domain, Std: protein standard Expected molecular weight of monomeric H7 rHA = 65 kDa, Expected molecular weight of trimeric H7 rHA = 194.8 kDa.*

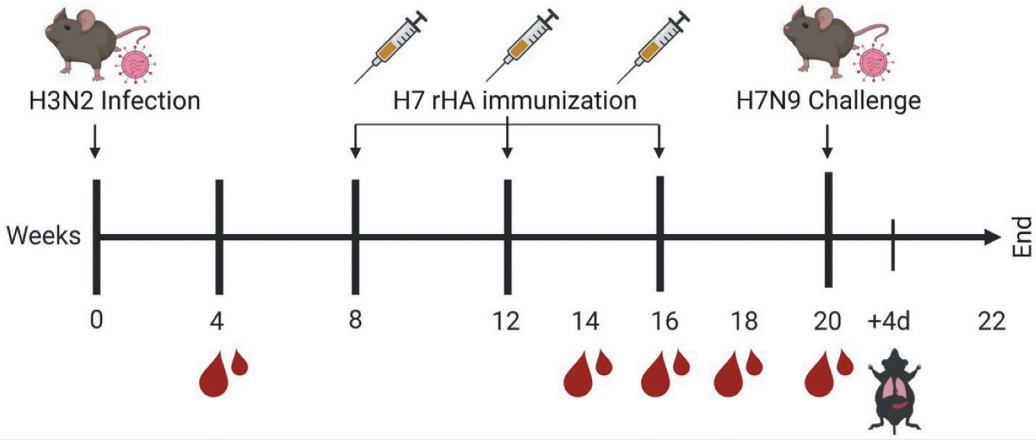

Group	Pre-immunization	Vaccination	Challenge	Number of animals
1. OPT1	HK/14 H3N2	OPT1 H7 rHA	Anh/13 H7N9	n=10
2. WT		WT H7 rHA		n=10
3. Preimmune control		None		n=11
4. Naïve control	None			n=12

Figure 2. Study design. In order to establish preexisting immunity, HLA-DR3 mice designated as OPT1, WT, and preimmune control groups were infected with sub-lethal dose of A/Hong Kong/4108/2014 (H3N2) via intranasal route ($1X10^6$ PFU/mouse). The establishment of preexisting immunity to H3N2 was confirmed by seroconversion at week 4. The mice of OPT1 and WT groups received three vaccines (3 µg of H7 rHA) without adjuvant at 4 week intervals via intramuscular route. The antibody response to vaccinations was monitored from serum collected at week 14, 16 and 18. At week 20, all mice were challenged with A/Anhui/1/2013 H7N9 (10 LD50) via intranasal route ($1X10^4$ PFU/mouse). Mice were monitored for clinical symptoms and weight loss for 12 d. At d 4, three mice were randomly selected from each group to assess viral lung titers.

0.05 ml/mouse) with A/Hong Kong/4108/2014 (H3N2) and divided into OPT1 (n = 10), WT (n = 10), and pre-immune /not immunized (n = 11) groups. Mice were intramuscularly injected 3X at four-week intervals with each vaccine (3 µg) without adjuvant beginning at 8 weeks post-infection (Figure 2). At week 20, all mice were transferred to a biosafety level 3 (BSL-3) facility for viral challenge. Mice were briefly anesthetized and infected with a 10 LD_{50} dose of A/Anhui/1/2013 H7N9 via intranasal route ($1X10^4$ PFU/0.05 ml) (Figure 2). At 4 d post-challenge, three mice in each group were randomly selected and sacrificed to harvest lung tissue (Figure 2). Remaining mice were monitored for clinical symptoms and euthanized at 12 d post-challenge (Figure 2). All procedures were in accordance with the NRC Guide for Care and Use of Laboratory Animals, the Animal Welfare act, and the CDC/NIH Biosafety and Microbiological and Biomedical Laboratories (IACUC # A2017 11–021-Y3-A11).

Mice were bled prior to study onset to determine seronegative status for both H3 and H7 and were bled again at week 4 to confirm H3-specific seroconversion following H3N2 infection (Figure 2). To evaluate the humoral response to each vaccination, blood was also collected at weeks 14, 16, 18, and 20 (Figure 2). Blood was collected via submandibular bleeding using a lancet and transferred to a microfuge tube. Tubes were incubated at room temperature for at least 30 min prior to centrifugation, sera were collected and frozen at −20°C ± 5°C.

Hemagglutination-Inhibition (HAI) assay

A hemagglutination inhibition assay (HAI) assay was used to assess receptor-blocking antibodies to the HA protein to inhibit the agglutination of turkey red blood cells (TRBCs). The protocol is taken from the CDC laboratory influenza surveillance manual. To inactivate nonspecific inhibitors, mouse sera was treated with receptor destroying enzyme (RDE, Denka Seiken, Co., Japan) prior to being tested. Three parts of RDE were added to one-part sera and incubated overnight at 37°C. The RDE was inactivated at 56°C for 30 min; when cooled, 6 parts of sterile PBS were added to the sera and were kept at 4°C until use. RDE treated sera was two-fold serially diluted in v-bottom microtiter plates. Twenty-five µl of virus at 8 HAU/50 µL was added to each well (4 HAU/25 µL). Plates were covered and incubated with virus for 20 min at room temperature before adding 0.8% TRBCs in PBS. The plates were mixed by agitation and covered; the RBCs were then allowed to settle for 1 h at room temperature. HAI titer was determined by the reciprocal dilution of the last well which contained non-agglutinated RBC. Negative and positive serum controls were included for each plate. All mice were negative (HAI < 1:10) for preexisting antibodies to currently circulating human influenza viruses prior to study onset.

Enzyme-linked immunosorbent assay (ELISA)

Immunolon 4BX ELISA plates (Thermo Life Sciences, Philadelphia, PA) were coated overnight at 4°C with 100 ng/well of rHA or anti-mouse IgG (γ-chain specific)–peroxidase antibody produced in goat in carbonate buffer (pH 9.4) with 250 ng/mL bovine serum albumin (BSA). The plates were blocked for 2 h at 37°C with blocking buffer (2% BSA, 1% gelatin in PBS/0.05% Tween 20). Serum samples were initially diluted 1:100 and then further serially diluted in 1:2 in blocking buffer. Serially diluted samples were added to the assay plate in duplicate and incubated overnight at 4°C. Plates were washed

three times with wash buffer (PBS with 0.05% Tween 20) and horseradish peroxidase (HRP)-conjugated goat anti-mouse IgG (Southern Biotech, Birmingham, AL, USA) at a 1:3000 dilution and incubated for 2 h at 37°C. Plates were washed 7 times with the wash buffer prior to development with 100 µL of 0.1% 2,2′-azino-bis(3-ethylbenzothiaozoline-6 – sulfonic acid; ABTS) solution with 0.05% H_2O_2 for 40 min at 37°C. The reaction was terminated with 1% (w/v) sodium dodecyl sulfate (SDS). Colorimetric absorbance at 414 nm was measured using a PowerWaveXS (Biotek, Winooski, VT, USA) plate reader. The magnitude of IgG responses among groups was analyzed by area under the curve (AUC) analysis using Prism (GraphPad Software).[14]

Plaque forming assay (PFA)

Viral titers were determined using a plaque-forming assay as previously using 1×10^6 Madin-Darby Canine Kidney (MDCK) cells, as previously described.[15] Briefly, lung tissue samples collected at 4 d post-challenge were snapped frozen and kept at −80°C until processing. Lung tissue was diluted (10° to 10^6) and overlayed onto confluent MDCK cell layers for 1 h in 200 µl of DMEM supplemented with penicillin–streptomycin. Cells were washed after 1-h incubation and DMEM was replaced with 3 mL of 1.2% Avicel (FMC BioPolymer; Philadelphia, PA) – MEM media supplemented with 1 µg/mL TPCK-treated trypsin. After 48 h incubation at 37°C with 5% CO2, the overlay was removed and washed 2x with sterile PBS, cells were fixed with 10%-buffered formalin and stained for 15 mins with 1% crystal violet. Cells were washed with tap water and allowed to dry. Plaques were counted and the plaque-forming units calculated (PFU/mL).

Statistical analysis

The difference in AUC data of anti-H7 rHA IgG response and lung viral titer among groups was analyzed by ordinary one-way ANOVA, followed by Tukey's multiple comparison test. The difference in body weight loss of each time point was tested by Repeated Measures one-way ANOVA followed by Tukey's multiple comparison test. All statistical analysis was performed using Prism (GraphPad Software). The statistical difference in challenged survival curve was determined by Lob-rank (Mantel-Cox) test (GraphPad Software).

Results

Optimized hemagglutinin vaccine development

Optimized T cell epitope-engineered H7 antigen (OPT1) was designed by replacing three amino acids in WT H7 $HA_{316\text{-}324}$.[8] The modifications replaced a T_{reg}-inducing epitope with a conserved promiscuous $CD4^+$ T effector epitope (Figure 1B). The OPT1 H7 HA sequence was expressed as soluble recombinant HA ectodomain followed by a GS linker followed by a GCN4 trimerization domain (Figure 1A).[16] An AviTag™ and a 6X HIS tag for detection and purification follow the trimerization domain (Figure 1B). H7 rHA expression was confirmed by SDS-PAGE and Western blot by using an anti-HIS antibody to the 6X HIS region located at the COOH-terminus of the protein (Figure 1C). Trimerization was confirmed by native PAGE that shows both OPT1 and WT H7 HA migrate according to their expected molecular weight of ~195 kDa (Figure 1D).

Vaccination of HLA-DR3 mice with optimized H7 rHA antigens

The MHC-II knock-out/HLA-DR3 knock-in transgenic (HLA-DR3) mice[8] were infected intranasally with the A/Hong Kong/4108/2014 (HK/14; H3N2) influenza virus (Figure 2). Pre-immunization was confirmed by HAI seroconversion (1:256–-1:1024) to HK/14 at week 4 post-infection (Figure 3A). There were no antibodies with cross-reactive HAI activity against the H7N9 A/Anhui/1/2013 (Anh/13) influenza virus (Figure 3B).

Mice were immunized without an adjuvant at weeks 8, 12, and 16 post-H3N2 influenza virus infection with either WT or OPT1 H7 HA vaccine (Figure 2). Mice that received either vaccine had no detectable anti-HA antibodies after the first vaccination (data not shown), but detectable titers were observed following the OPT1 H7 HA booster immunization (Figure 4A, B). Three mice in the OPT1 H7 HA group had a significant increase in anti-H7 rHA IgG titer after the third vaccination (Figure 4C). There was a statistically significant increase in the anti-HA H7 antibody titers in mice following three vaccinations with OPT1 (Figure 4D). One serum sample with the highest anti-H7 rHA IgG titer ($Abs_{414(sample\text{-}blank)}$ >0.7 in Figure 4C) also had H7N9 HAI activity (32 HAI units, data not shown). The WT H7 rHA-vaccinated mice responded poorly to vaccination and the anti-H7 rHA IgG titer was not significantly different compared to unvaccinated animals, both pre-immune and naïve controls (Figure 4C, D).

Viral challenge and lung viral titers

Mice were challenged with a lethal dose of A/Anhui/1/2013 (H7N9) (10e+4pfu/mouse/0.05 ml) and observed for survival, weight loss, and lung viral titers. All naïve mice lost >20% body weight following challenge. Only one survivor from the naïve control group regained weight. Mice vaccinated with OPT1 H7 HA vaccine had a higher survival rate than mice vaccinated with WT H7 rHA, unvaccinated H3N2 pre-immune, or naïve control groups (Figure 5A). Mice that received OPT1 H7 rHA showed >70% survival, while only one mouse (12%) in each pre-immune and naïve control group survived (Figure 5A). Approximately 30% of the mice vaccinated with WT H7 rHA vaccine survived challenge. Naïve mice had a rapid decline in body weight to d 10 post-infection (Figure 5B). Pre-immune mice vaccinated with the wtH7 HA, OPT1 H7 HA or unvaccinated lost between 10% and 15% of their body weight by d 7 post-infection. Mice that survived regained body weight over the next week (Figure 5B). The H7 OPT1 HA vaccination significantly improved the survival rate ($p = .0136$) and clinical sequel than WT H7 HA vaccine. The OPT1 H7 HA vaccinated mice had less severe clinical squeal following challenge. As a result, while most of the mice vaccinated with the WT HA or the naïve control lost more than 10% of body weight but

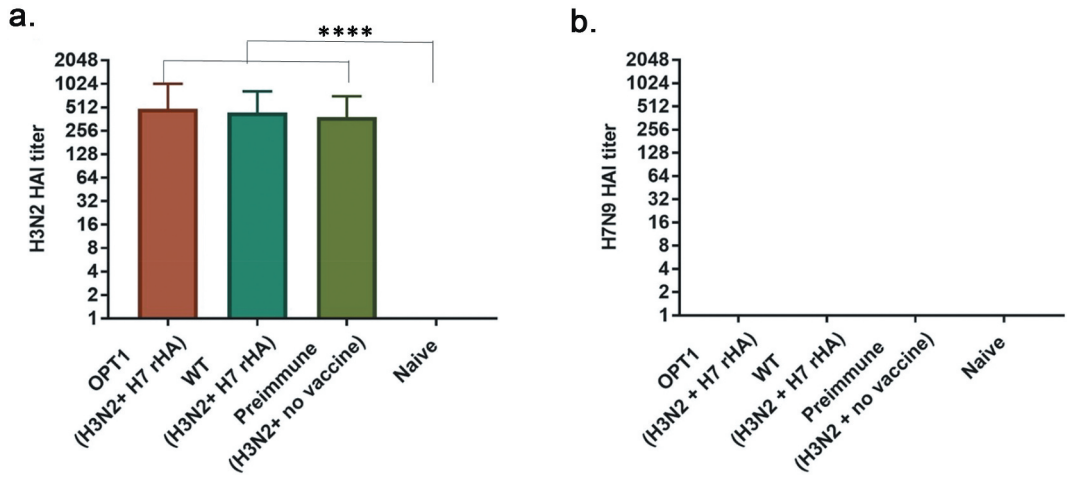

Figure 3. Seroconversion by the H3 pre-immunization. Serum samples were collected at four weeks after pre-immunization with A/Hong Kong/4801/2014 (H3N2) virus (week 4). Seroconversion was determined by the presence of hemagglutination inhibition ability to 8 HAu of A/Hong Kong/4801/2014 (H3N2) virus (A). The serum samples were also tested for the cross-reactivity to A/Anhui/1/2013 (H7N9) virus (B). Data is presented as the mean (± SD) of HAI titer.

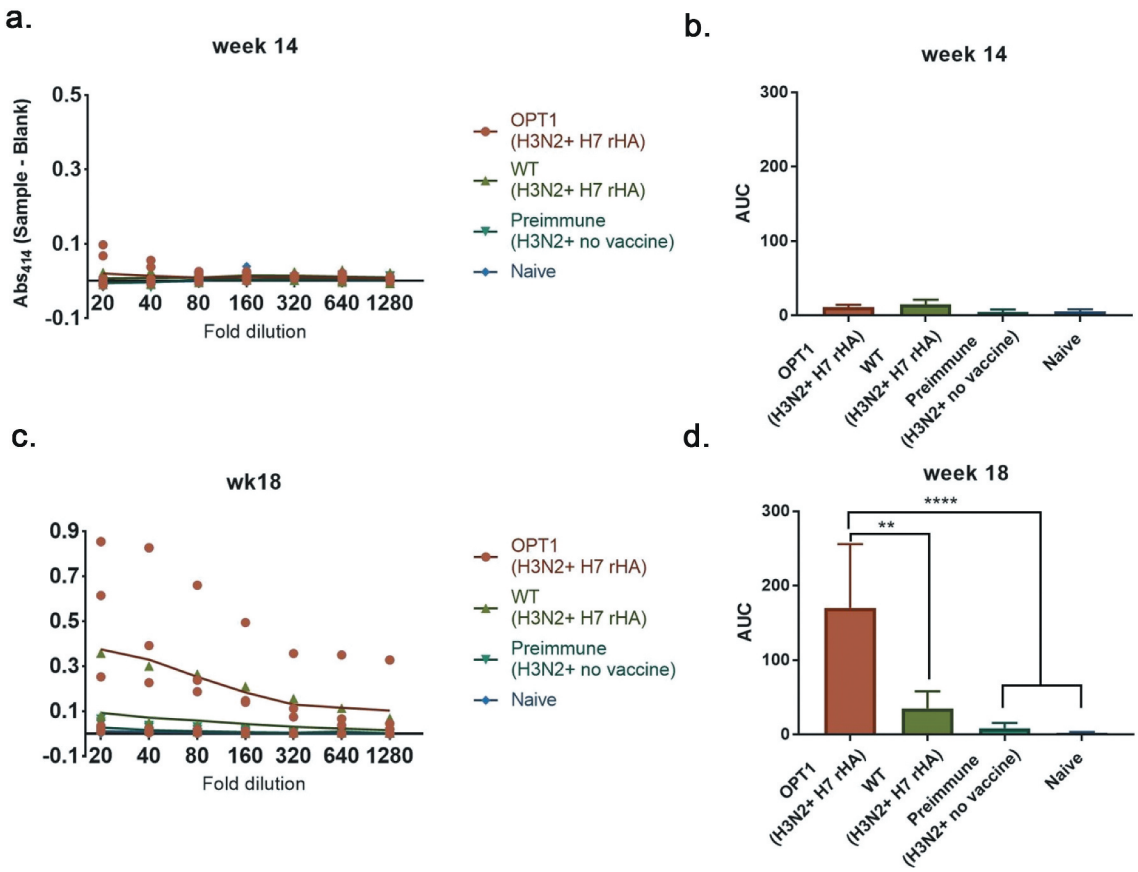

Figure 4. H7 rHA specific IgG response to vaccinations. Serum samples were collected at two weeks after 2nd and 3rd vaccination (week 13 and 17, respectively) and were evaluated for IgG antibody reactivity against the H7 rHA derived from A/Anhui/1/2013 H7N9 by ELISA. Data is presented as individual plot of absorbance at 414 nm (A and C) and the mean (± SD) of Area under the curve(AUC) values (B and D). *$p < .05$, **$p < .005$, ****$p < .0001$.

almost all of these mice regained their weight by the end of study. Similar results were observed in pre-immune mice. Meanwhile, 43% of OPT1 H7 HA vaccinated mice maintained 90% of their original body weight and those that survived recovered. Since the only difference between WT H7 and OPT1 H7 HA was the three amino acids in the targeted sequence, this epitope modification appears to be the major reason for improved protection by OPT1 H7 HA vaccine.

There was no significant difference in the lung viral titers between naïve and pre-immune control mice (Figure 5C). Mice had an average viral lung titer of 10e+6 pfu/ml at 4 d post-infection. The average viral lung titer from mice vaccinated with WT H7 rHA was similar to the titers from both unvaccinated controls, except for a 1-$\log_{10}$ reduction observed in a single WT H7 HA vaccinated mouse (Figure 5C). In comparison, mice vaccinated with H7 OPT1 HA vaccine had an

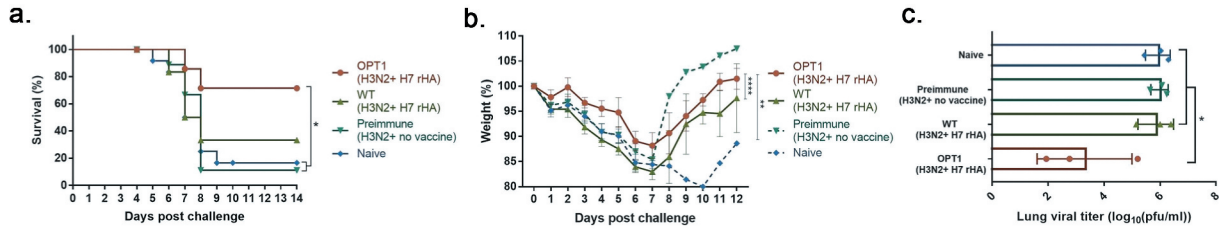

Figure 5. Lethal H7N9 influenza virus challenge of mice. HLA-DR3 mice (10–12 mice/group) pre-immunized with H3N2 A/Hong Kong/4801/2014 (H3N2) at week 0 and vaccinated at weeks 8, 12 and 16 weeks with rH7 HA without adjuvant. At week 20, mice were intranasally infected with 10e+4 PFU of the A/Anhui/1/2013 H7N9) virus. Mice were monitored daily for weight loss (A and B) and viral lung titers in selected mice 4 d post challenge (C). Weight loss and lung viral titer was presented as mean± standard deviation (B and C). The weight loss data from a single survived mouse was marked as dotted line (B; preimmune and naïve groups). *$p < .05$, **$p < .01$, ***$p < .001$, ****$p < .0001$.

average viral lung titer of 1–3 $\log_{10}$ lower than pre-immune or naïve control mice (Figure 5C). Overall, the optimized H7 rHA vaccine elicited greater protection against viral challenge than mice vaccinated with the WT H7 rHA.

Discussion

The H7 hemagglutinin is poorly immunogenic in both natural infection and vaccination studies[17,18]. With the inclusion of adjuvants, as well as multiple vaccine doses, the immunogenicity of H7 HA vaccines can be improved. In a recent Phase II clinical study, two-doses of Panblok H7 HA plus the AS03 adjuvant elicited seroconversion by d 50 post-vaccination in almost all participants.[19] However, there was a sharp decline in anti-H7 HA serum antibody and by d 211 more than half of the responders were seronegative. As with most vaccine formulations, addition of an adjuvant may increase risk complications, which can seriously impede the vaccine approval process and raise adverse events and public acceptance of a new vaccine. In this trial, there was a significant number of participants that had minor adverse events, including fatigue (16–30%), injection site erythema (3–11%), and myalgia (13–31%). Thus, for the development of safe and efficacious H7 HA vaccines, it may be necessary to search for alternative strategies to improve H7 HA immunogenicity. This study demonstrates a promising strategy to improve the immunogenicity of H7 HA without the use of adjuvants. The H7 HA carries more frequent immunosuppressive motifs, designated as regulatory T cell epitopes (Tregs) that are primarily located in the HA2 stalk domain. H7 HA stalk domains have inhibitory effects on the elicitation of neutralizing antibodies against the HA head domain.[20] Vaccine strategies that excluded the HA2 stalk domain from an Fc-conjugated HA-based influenza vaccine were more effective at eliciting neutralizing antibodies.[20] Replacing the transmembrane domain (TM) of H7 HA with a TM from an H3 HA antigen increased antibody titers and broadened the range of protection against H7N9 influenza virus infection.[21] The replacement of immunosuppressive motifs in the HA2 stalk domain is an effective approach to improve the poor immunogenicity of H7 HA proteins.

The CD4 + T cell response is not crucial to provide protection against influenza virus infection in mice when there are intact CD8 + T cells and B cells.[22] However, CD4 + T cell responses are critical for the development of memory CD8 + T cells, as well as assist in class-switching, affinity maturation, differentiation into antibody-producing B cells, and the formation of antigen-specific memory.[23] Conserved CD4 + T cell epitopes found from multiple seasonal influenza subtypes provide cross-protection to all 16 HA influenza A subtypes.[24] A robust engagement of $CD4^+$ T cells is a key priority in H7 vaccine development. Therefore, the conversion of naïve cells into the memory cells is critical in protection against this novel pathogen.

In order to develop an optimized H7 HA vaccine candidate, *in silico* immunoinformatic tools identified putative T_{reg} epitopes that were replaced with conserved CD4 + T cell epitopes originating from seasonal influenza strains.[6] This modification was aimed to recruit the help of H3-specific $CD4^+$ memory T cells, while limiting tolerogenic responses introduced by T_{reg} activation, and to promote a robust anti-H7 HA immune responses.[25] Through the application of *in silico* immunoinformatic tools, one of putative Treg epitopes in the H7 $HA_{316\text{-}324}$ was identified. This epitope had high similarity with conserved CD4+ stimulating epitope, H3 $HA_{322\text{-}345}$.[7] This led to the identification of a highly conserved, HLA-binding 9-mer, predicted to be significantly more immunogenic than its H7 homolog that resulted in the replacement of three amino acids of H7 $HA_{316\text{-}324}$ peptide[25] and the new HA vaccine candidate was designed H7 OPT1 HA.[8]

The OPT1 H7 HA vaccine enhanced serum IgG titers following vaccination in a humanized mouse model utilizing immune-deficient mice reconstituted with PBMCs from human donors (with presumed seasonal influenza-history). However, in this earlier report, protection against viral challenge was not determined.[8] Therefore, in this study, it was hypothesized that the enhanced immunogenicity of immune-engineered H7 HA could protect mice from the stringent avian H7N9 challenge with a history of H3N2 influenza virus exposure. Establishing a pre-immune state is integral to establishing a memory T cell pool that can be harnessed through the engineered epitope to drive a more efficient response than by mobilization of the naïve compartment alone. Our initial study in immunodeficient mice introduced HLA-expressing antigen-presenting cells from human donors. For this reason, H7 HA vaccination and H7N9 lethal challenge were studied in a transgenic mouse model where HLA restriction and immune history could be controlled, even if mouse TCR repertoires are less diverse than in humans. These mice expressed the DR3 supertype allele and *in silico* analysis predicted that both the endogenous H7 T_{reg}-inducing epitope and H3-derived effector

T cell epitope would bind this allele. The underlying mechanism of the protection remains to be determined, but the full efficacy of H7 OPT1 HA vaccine should be mediated by more than just the DR3-mediated response. Mice reconstituted with human PBMCs, had a 5-fold higher serum IgG titer and a 20-fold greater anti-H7-HA B cell frequency than mice vaccinated with WT H7 HA vaccines.[8] The WT H7 HA expanded $CD25^{high}$FoxP3+ CD4 + T cells in human PBMC cultures that are associated with an immunosuppressive motif in the HA that results in suppressed effector T-cell responses.[26] The significance of these results was that the enhancement of antibody titers could be achieved by epitope modification. Antibody enhancement could be achieved in a murine model despite limited immune history and T-cell diversity compared to human PBMCs, and therefore enhancement of the immune responses was correlated with protection.

Currently, many groups are testing influenza virus vaccine candidates to meet the challenge of developing a vaccine that elicits broadly reactive and long-lasting protective immune responses. Commonly, these experimental vaccines are tested in naive animal models that do not have anti-influenza immunity. However, humans have preexisting immunity to influenza viral antigens, particularly antibodies to the HA and NA glycoproteins. Influenza A viruses can be categorized into two phylogenetic groups (group 1 and group 2).[27] Group 1 influenza viruses include H1, H2, and H5 subtypes and the group 2 viruses are exemplified by the H3 and H7 subtypes.[27] H3N2 influenza viruses entered the human populations during the pandemic of 1968 and have co-circulated in people causing seasonal infections in the human population each year.[28] Adults under the age of 50 y were most likely imprinted with a memory B and T cell population by an H3N2 virus infection.[28] Therefore, to better model human immune history, DR3 mice were infected with an H3N2 influenza virus, resulting in seroconversion. These H3 HA elicited antibodies do not cross-reactive HAI activity against the WT H7 HA (Figure 3). However, following vaccination, there was a statistically significant improvement in total serum anti-HA IgG, reduction in weight loss, and mortality after the avian H7N9 challenge in mice vaccinated with the Opt1 H7 HA vaccine compared to mice vaccinated with the WT H7 HA vaccine.

Most vaccinated mice were protected against avian H7N9 viral challenge without any detectable HAI titers. Antibodies and memory B cells directed against the conserved HA stem region are prevalent in humans, but their levels are much lower than B cell responses directed to variable epitopes in the HA head.[29] Antibodies to the HA stalk, and not the HA head domain, are increased following vaccination with two different vaccines from the same group with mismatched HA head regions. Indeed, immunization of humans with the avian influenza virus H5N1 induced broadly cross-reactive HA stem-specific antibodies.[30,31] Currently, there are vaccine strategies using heterologous influenza HA immunizations to increase the levels of broadly neutralizing antibodies and for priming the human population to respond quickly to emerging pandemic influenza threats. The Opt1 H7 HA vaccine was most effective in eliciting anti-HA antibodies in H3N2 pre-immune mice. These mice had higher titer antibodies, presumably directed against the stem, than pre-immune mice vaccinated with the WT HA vaccine (Figure 4). Broadly reactive antibodies specific for the HA stem have biological activities other than direct virus neutralization, such as antibody-dependent cellular cytotoxicity (ADCC). Therefore, the use of these enhanced HA vaccines may increase these types of antibody activities directed to the HA stem region. Future studies will need to assess the true mechanism(s).

A previous study conducted by Wada *et al.* showed that in a conventional mouse model, the immunogenicity of H7 and H3 HA was observed in similar levels,[8] which is not consistent with their relative immunogenicity observed in humans. Only in a humanized mouse model, the NOD/SCID/Jak3−/− (NOJ) mouse reconstituted with human PBMCs, did the H7 HA elicit lower immunogenicity, especially in comparison to the immunity elicited by H3 rHA.[8] The HLA-DR3 transgenic mouse model is one of the best models for this examining CD4 + T cell responses that are completely restricted to human MHC II.[4] However, HLA-DR3 transgenic mice have inherent limitations in order to emulate human MHC II – TCR interactions such as (1) the HLA-DR3 transgenic mouse only reflects a portion of highly polymorphic MHC II and (2) the origin of the CD4 + T cells is still completely from mouse. Most likely due to these limitations, not all mice in the OPT1 HA vaccine group elicited antibodies following vaccination. Approximately 50% of mice vaccinated with OPT1 H7 rHA exhibited the same titer pre- and post-vaccination. It is not clear how critical those limitations are to elicit productive T cell responses, but it is possible that subtle incompatibilities could have interrupted the MHC II-TCR interaction. To overcome the limitations of transgenic mice, recent studies applied human organ engraphed mouse models, such as BLT (bone marrow-liver-thymus) and Hu-HSC (human hematopoietic stem cell) mice [27]. However, the application of such models might not be practical unless the impact of aforementioned limitations is clearly identified.

The relative size and diversity of the H3 HA-specific memory cell population induced by the H3N2 viral infection may have been suboptimal for the detection of immune responses directed against the CD4 + T cell motifs embedded in OPT1 H7 HA proteins. All pre-immunized mice elicited H3N2-specific HAI antibody titers (Figure 3A). However, these types of antibodies do not guarantee that the mice developed memory response the target motifs originated from the stem region of the H3 HA protein. Further, enhancing immunogenicity with adjuvants or a modified regimen may be a method for developing stronger H3N2-directed memory. Therefore, future pre-immune studies should focus on increasing $CD4^+$ T cell frequencies with repeated H3-HA exposures, either through infection or immunization. Increased H3N2 influenza virus history may a better model of human exposure to viral antigens, as people experience multiple exposures to H3N2 influenza and/or receive prophylactic immunizations annually.

Overall, the results from this study validate the T cell epitope-guided antigen engineering approach as OPT1 H7 HA reduces disease severity and significantly enhances protection against lethal avian H7N9 challenge. Therefore, the underlying mechanism of the protection remains to be determined. Mice vaccinated with H7 OPT1 HA did have enhanced anti-HA serum IgG titers, which suggests that the non-neutralizing antibodies may play an important role in protection. Collectively, the protection

conferred by the T cell epitope-engineered H7 HA vaccines are able to elicit higher titer non-neutralizing and neutralizing antibodies, reduce Treg responses, stimulate CD4 + T cell responses, and subsequently enhance B cell responses. To investigate the underlying mechanisms, future studies should focus on detecting corresponding cell-mediated immune responses that might not be directly matched with the previous findings. This study translates the *in silico* hypothesis with the *in vivo* effectiveness.

Disclosure of potential conflicts of interest

No potential conflicts of interest were disclosed.

Funding

This work was supported by the National Institute of Allergy and Infectious Diseases (US) [R01AI132205].

References

1. Yu D, Xiang G, Zhu W, Lei X, Li B, Meng Y, Yang L, Jiao H, Li X, Huang W, et al. The re-emergence of highly pathogenic avian influenza H7N9 viruses in humans in mainland china, 2019. Euro Surveillance: Bulletin Europeen Sur Les Maladies Transmissibles = European Communicable Disease Bulletin. 2019;24(21):1900273.
2. Fineberg HV. Pandemic preparedness and response–lessons from the H1N1 influenza of 2009. N Engl J Med. 2014;370:1335–42.
3. Jackson LA, Campbell JD, Frey SE, Edwards KM, Keitel WA, Kotloff KL, Berry AA, Graham I, Atmar RL, Creech CB, et al. Effect of varying doses of a monovalent H7N9 influenza vaccine with and without AS03 and MF59 adjuvants on immune response: A randomized clinical trial. JAMA. 2015;314(3):237–46.
4. De Groot AS, Ardito M, Terry F, Levitz L, Ross T, Moise L, Martin W. Low immunogenicity predicted for emerging avian-origin H7N9: implication for influenza vaccine design. Hum Vaccin Immunother. 2013;9:950–56.
5. Richards KA, Nayak J, Chaves FA, DiPiazza A, Knowlden ZA, Alam S, Treanor JJ, Sant AJ. Seasonal influenza can poise hosts for cd4 t-cell immunity to H7N9 avian influenza. J Infect Dis. 2015;212:86–94.
6. Liu R, Moise L, Tassone R, Gutierrez AH, Terry FE, Sangare K, Ardito MT, Martin WD, De Groot AS. H7N9 t-cell epitopes that mimic human sequences are less immunogenic and may induce Treg-mediated tolerance. Hum Vaccin Immunother. 2015;11:2241–52.
7. Moise LBMB, Boyle CM, Kurt YN, Jang H, Schiffer CTMR, Martin WD, De Groot AS. T cell epitope engineering: an avian H7N9 influenza vaccine strategy for pandemic preparedness and response. Hum Vaccin Immunother. 2018;14:2203–07.
8. Wada Y, Nithichanon A, Nobusawa E, Moise L, Martin WD, Yamamoto N, Terahara K, Hagiwara H, Odagiri T, Tashiro M, et al. A humanized mouse model identifies key amino acids for low immunogenicity of H7N9 vaccines. Sci Rep. 2017;7(1):1283.
9. Gao R, Cao B, Hu Y, Feng Z, Wang D, Hu W, Chen J, Jie Z, Qiu H, Xu K, et al. Human infection with a novel avian-origin influenza a (H7N9) virus. N Engl J Med. 2013;368(20):1888–97.
10. Moise L, Gutierrez A, Kibria F, Martin R, Tassone R, Liu R, Terry F, Martin B, De Groot AS. Ivax: an integrated toolkit for the selection and optimization of antigens and the design of epitope-driven vaccines. Hum Vaccin Immunother. 2015;11:2312–21.
11. Weldon WC, Wang B-Z, Martin MP, Koutsonanos DG, Skountzou I, Compans RW. Enhanced immunogenicity of stabilized trimeric soluble influenza hemagglutinin. PloS One. 2010;5:e12466.
12. Kirchenbaum GA, Allen JD, Layman TS, Sautto GA, Ross TM. Infection of ferrets with influenza virus elicits a light chain-biased antibody response against hemagglutinin. J Immunol. 2017;199:3798–807.
13. Carter DM, Darby CA, Lefoley BC, Crevar CJ, Alefantis T, Oomen R, Anderson SF, Strugnell T, Cortés-Garcia G, Vogel TU, et al. Design and characterization of a computationally optimized broadly reactive hemagglutinin vaccine for H1N1 influenza viruses. J Virol. 2016;90(9):4720.
14. Angeletti D, Gibbs JS, Angel M, Kosik I, Hickman HD, Frank GM, Das SR, Wheatley AK, Prabhakaran M, Leggat DJ, et al. Defining b cell immunodominance to viruses. Nat. Immunol. 2017;18(4):456–63.
15. Matrosovich M, Matrosovich T, Garten W, Klenk HD. New low-viscosity overlay medium for viral plaque assays. Virol J. 2006;3(63).
16. Harbury PB, Zhang T, Kim PS, Alber T. A switch between two-, three-, and four-stranded coiled coils in GCN4 leucine zipper mutants. Science. 1993;262:1401.
17. Guo L, Zhang X, Ren L, Yu X, Chen L, Zhou H, Gao X, Teng Z, Li J, Hu J, et al. Human antibody responses to avian influenza a(H7N9) virus, 2013. Emerg Infect Dis. 2014;20(2):192–200.
18. Lee AC, Zhu H, Zhang AJ, Li C, Wang P, Li C, Chen H, Hung IF, To KK, Yuen KY. Suboptimal humoral immune response against influenza a(H7N9) virus is related to its internal genes. Clin Vaccine Immunol. 2015;22:1235–43.
19. ClinicalTrials.gov [Internet]. 2017 Sep 14. Identifier NCT03283319, Panblok H7 vaccine adjuvanted with AS03 or MF59. Bethesda (MD): National Library of Medicine (US); 2020 May 6 [Cited 2020 Jun 01]; Available from: https://clinicaltrials.gov/ct2/show/study/NCT03283319
20. He B, Xia S, Yu F, Fu Y, Li W, Wang Q, Lu L, Jiang S. Putative suppressing effect of igg Fc-conjugated haemagglutinin (HA) stalk of influenza virus H7N9 on the neutralizing immunogenicity of Fc-conjugated ha head: implication for rational design of HA-based influenza vaccines. J Gen Virol. 2016;97:327–33.
21. Wang Y, Wu J, Xue C, Wu Z, Lin Y, Wei Y, Wei X, Qin J, Zhang Y, Wen Z, et al. A recombinant H7N9 influenza vaccine with the H7 hemagglutinin transmembrane domain replaced by the H3 domain induces increased cross-reactive antibodies and improved interclade protection in mice. Antiviral Res. 2017;143:97–105.
22. Brown DM, Roman E, Swain SL. CD4 T cell responses to influenza infection. Semin Immunol. 2004;16:171–77.
23. Laidlaw BJ, Craft JE, Kaech SM. The multifaceted role of CD4(+) T cells in CD8(+) T cell memory. Nature Reviews. Immunology. 2016;16:102–11.
24. Babon JA, Cruz J, Ennis FA, Yin L, Terajima M. A human CD4+ T cell epitope in the influenza hemagglutinin is cross-reactive to influenza a virus subtypes and to influenza b virus. J Virol. 2012;86:9233–43.
25. Russell RJ, Kerry PS, Stevens DJ, Steinhauer DA, Martin SR, Gamblin SJ, Skehel JJ. Structure of influenza hemagglutinin in complex with an inhibitor of membrane fusion. PNAS. 2008;105:17736.
26. Liu R, Moise L, Tassone R, Gutierrez AH, Terry FE, Sangare K, Ardito MT, Martin WD, De Groot AS. H7N9 T-cell epitopes that mimic human sequences are less immunogenic and may induce Treg-mediated tolerance. Hum Vaccin Immunother. 2015;11:2241–52.
27. Joyce MG, Wheatley AK, Thomas PV, Chuang GY, Soto C, Bailer RT, Druz A, Georgiev IS, Gillespie RA, Kanekiyo M, et al. Vaccine-induced antibodies that neutralize group 1 and group 2 influenza a viruses. Cell. 2016;166(3):609–23.

28. Gostic KM, Ambrose M, Worobey M, Lloyd-Smith JO. Potent protection against H5N1 and H7N9 influenza via childhood hemagglutinin imprinting. Science. 2016;354:722.
29. Neu KE, Henry Dunand CJ, Wilson PC. Heads, stalks and everything else: how can antibodies eradicate influenza as a human disease? Curr Opin Immunol. 2016;42:48–55.
30. Ellebedy AH, Krammer F, Li GM, Miller MS, Chiu C, Wrammert J, Chang CY, Davis CW, McCausland M, Elbein R, et al. Induction of broadly cross-reactive antibody responses to the influenza HA stem region following H5N1 vaccination in humans. PNAS. 2014;111(36):13133–38.
31. Wheatley AK, Whittle JR, Lingwood D, Kanekiyo M, Yassine HM, Ma SS, Narpala SR, Prabhakaran MS, Matus-Nicodemos RA, Bailer RT, et al. H5N1 vaccine-elicited memory B cells are genetically constrained by the IGHV locus in the recognition of a neutralizing epitope in the hemagglutinin stem. J Immunol. 2015;195(2):602–10.